

Controlling nonlinear PDEs using low-dimensional bilinear approximations obtained from data

Sebastian Peitz¹

¹Department of Mathematics, Paderborn University, Germany

June 6, 2022

Abstract

In a recent article we presented a framework to control nonlinear partial differential equations (PDEs) by means of Koopman operator based reduced models and concepts from switched systems. The main idea was to interpret a control system as a set of autonomous systems for which the optimal switching sequence has to be computed. These individual systems can be approximated by reduced order models obtained from data, and one can guarantee convergence under certain assumptions. In this article we extend these results to continuous control inputs using linear interpolation between two Koopman operators corresponding to constant controls, which results in a bilinear control system. Although convergence can be proved when the PDE depends linearly on the control, we show that this approach is also valid in other scenarios using a flow control example.

1 Introduction

The increasing complexity of technical systems presents a great challenge for control, in particular if the system dynamics is described by partial differential equations (PDEs). This is even more challenging for nonlinear systems, see [BN15] for a recent survey on turbulent flow control. To this end, advanced control techniques such as *Model Predictive Control (MPC)* [GP17] or machine learning based control [DBN17, Kut17] have gained more and more attention in recent years. In MPC, an open-loop optimal control is computed repeatedly on a finite-time horizon using a model of the system dynamics. This results in a closed-loop control behavior but requires solving the open-loop problem in a very short time, which is in general infeasible for nonlinear PDEs when using a standard discretization approach such as finite elements or finite volumes.

To overcome this problem, the high fidelity model can be replaced by a surrogate model which can be solved much faster, see [LMQR14, BGW15] for overviews. Various methods exist for deriving such a surrogate model, the most common for nonlinear systems probably being *Galerkin projection* in combination with *Proper Orthogonal Decomposition (POD)* [Sir87]. Many researchers are working on optimal control methods based on POD for which convergence towards the true optimum can

be shown, either using the singular values associated with the POD modes [KV99, Row05, HV05, TV09, BDPV17] or by *trust-region* approaches [Fah00, BC08, QGVW16, RTV17, Pei17]. However the applicability of POD models has limitations, in particular for complicated system dynamics.

An alternative approach to construct a *reduced order model (ROM)* is by means of the *Koopman operator* [Koo31] which is a linear but infinite-dimensional operator describing the dynamics of observables. This approach can even be applied to sensor measurements or in situations where the underlying system dynamics is unknown. A lot of work has been invested both to study the properties of the Koopman operator [MB04, Mez05, BMM12, Mez13] as well as to efficiently compute numerical approximations via *Dynamic Mode Decomposition (DMD)* or *Extended Dynamic Mode Decomposition (EDMD)* [Sch10, RMB⁺09, TRL⁺14, WKR15, KGPS16, KKS16]. More recently, various attempts have been made to use ROMs based on the Koopman operator for control problems [PBK15, PBK16, BBPK16, KM16, KKB17]. In many of these approaches, the Koopman operator is approximated for an augmented state (consisting of the actual state and the control) in order to deal with the non-autonomous control system. For this reason, a very large amount of data is necessary to cover a sufficient range of the dynamics.

An alternative approach has been presented in [PK17], where the control system is replaced by a set of autonomous systems with constant control inputs. This way, the optimal control problem is transformed into a switching time problem (cf. e.g. [SOBG16]), and convergence towards the true optimum can be shown by utilizing recent convergence results for EDMD [AM17, KM17]. In this article, we extend these results in such a way that we obtain a bilinear control system [BDK74, Eli09]. Instead of switching between the autonomous dynamics, we also allow intermediate control values. In the reduced model, these controls are realized by linear interpolation between the different Koopman operators. If the control system depends linearly on the input, one can prove convergence of the ROM based optimal control problem towards the true optimum. Embedded in an MPC framework, we observe that the approach also yields remarkable results for nonlinear control dependencies. The examples we consider range from a simple two-dimensional nonlinear system over the 1D Burgers equation to the 2D Navier–Stokes equations.

The remainder of the article is structured as follows. In Section 2, we introduce basic concepts for the Koopman operator and its numerical approximation as well as the switching time control approach. The extension to continuous control inputs is then introduced in Section 3 and the application to reduced order modeling of PDEs is discussed in Section 4. Finally, the combination with MPC is addressed in Section 5 before we conclude with a short summary and possible future directions in Section 6.

2 Koopman Operator based reduced order models

Let $\Phi : \mathcal{M} \rightarrow \mathcal{M}$ be a discrete deterministic dynamical system defined on the state space \mathcal{M}^1 and let $f : \mathcal{M} \rightarrow \mathbb{R}$ be a real-valued observable of the system. (An extension to vector-valued observables can be realized in a straightforward manner [BMM12].) Then the Koopman operator $\mathcal{K} : \mathcal{F} \rightarrow \mathcal{F}$ with $\mathcal{F} = L^\infty(\mathcal{M})$, which describes the evolution of the observable f , is defined by

$$(\mathcal{K}f)(y) = f(\Phi(y)),$$

¹The state space \mathcal{M} can either be a finite-dimensional (i.e., $\mathcal{M} \subseteq \mathbb{R}^d$) or an infinite-dimensional space [KM17].

see [BMM12, Mez13, WKR15] for more details. The Koopman operator is linear but infinite-dimensional. Its adjoint, the Perron–Frobenius operator, describes the evolution of densities. The definition of the Koopman operator can be naturally extended to continuous-time dynamical systems as described in [LM94, BMM12]. Given an autonomous PDE of the form

$$\dot{y}(x, t) = G(y(x, t)),$$

the *Koopman semigroup* of operators $\{\mathcal{K}^t\}$ is defined as

$$(\mathcal{K}^t f)(y) = f(\Phi^t(y)),$$

where Φ^t is the flow map associated with G . In what follows, we will mainly consider discrete dynamical systems, given by the discretization of ODEs or PDEs. That is, $\Phi = \Phi^h$ for a fixed time step h .

2.1 Extended Dynamic Mode Decomposition

Dynamic Mode Decomposition (DMD) was initially proposed by Peter Schmid [Sch10] (see also [TRL⁺14]). It is a modal decomposition method for large data sets such as fluid flow simulations (see [TBD⁺17] for an overview of different modal decomposition methods). While it is similar to Proper Orthogonal Decomposition (POD) [Sir87], the main difference is that instead of obtaining a basis with the optimal projection error, each of the DMD modes possesses a frequency with which it oscillates, determined by the corresponding complex eigenvalue [RMB⁺09]. Consequently, DMD can be interpreted as a generalized Fourier transform.

Extended Dynamic Mode Decomposition (EDMD) [WKR15, KKS16] is a generalization of DMD and can be used to compute a finite-dimensional approximation of the Koopman operator, its eigenvalues, eigenfunctions, and modes. The following brief description of EDMD is based on the review paper [KNK⁺17]. EDMD constructs an approximation of the Koopman operator from data (i.e. measurements) given by $z = f(y) \in \mathbb{R}^q$. For finite-dimensional systems, it is possible to observe the full state (*full state observable*) but the approach is valid for arbitrary observables. In contrast to DMD, in EDMD the observations can be expressed in terms of arbitrary basis functions (e.g. monomials, Hermite polynomials or radial basis functions). For a given set of basis functions $\{\psi_1, \psi_2, \dots, \psi_k\}$ (a so-called *dictionary*), we define $\psi: \mathbb{R}^q \rightarrow \mathbb{R}^k$ by

$$\psi(z) = [\psi_1(z) \quad \psi_2(z) \quad \dots \quad \psi_k(z)]^\top.$$

If $\psi(z) = z$, we obtain DMD as a special case of EDMD. We assume that we have either measurement or simulation data, written in matrix form as

$$Z = [z_1 \quad z_2 \quad \dots \quad z_m] \quad \text{and} \quad \tilde{Z} = [\tilde{z}_1 \quad \tilde{z}_2 \quad \dots \quad \tilde{z}_m],$$

where $\tilde{z}_i = f(\Phi(y_i))$. The data can either be obtained via many short simulations or experiments with different initial conditions or one long-term trajectory or measurement. If the data is extracted from one long trajectory, then $\tilde{z}_i = z_{i+1}$. The data matrices are embedded into the typically higher-dimensional feature space by

$$\Psi_Z = [\psi(z_1) \quad \psi(z_2) \quad \dots \quad \psi(z_m)] \quad \text{and} \quad \Psi_{\tilde{Z}} = [\psi(\tilde{z}_1) \quad \psi(\tilde{z}_2) \quad \dots \quad \psi(\tilde{z}_m)].$$

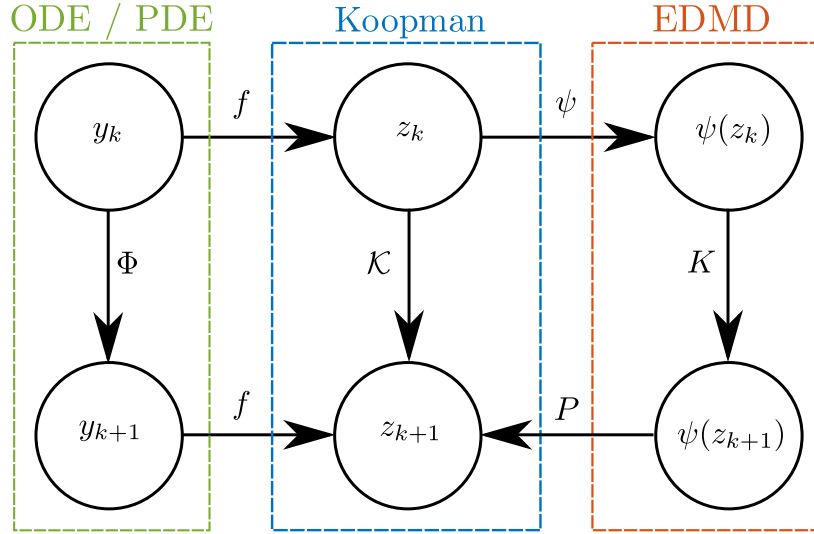


Figure 1: Relation between the system dynamics Φ , the corresponding Koopman operator \mathcal{K} and its finite-dimensional representation K computed via EDMD.

With these data matrices, we then compute the matrix $K \in \mathbb{R}^{k \times k}$ defined by

$$K^\top = \Psi_{\tilde{Z}} \Psi_Z^+ = (\Psi_{\tilde{Z}} \Psi_Z^\top) (\Psi_Z \Psi_Z^\top)^+.$$

The matrix K can be viewed as a finite-dimensional approximation of the Koopman operator. The decomposition of the Koopman operator into eigenvalues, eigenfunctions, and modes is commonly used to analyze the system dynamics as well as predict the future state. In the situation we are interested in here, we can choose an even simpler approach and compute updates for the observable z directly using K :

$$\psi(z_{i+1}) = K^\top \psi(z_i), \quad i = 0, 1, \dots$$

From here, we can obtain z_{i+1} using the projection matrix P , cf. Figure 1, where the relation between the dynamical system Φ , the related Koopman operator \mathcal{K} , and the EDMD approximation K is visualized.

2.2 Convergence of EDMD towards the Koopman operator

First results showing convergence of the EDMD algorithm towards the Koopman operator have recently been proved in [AM17, KM17]. In short, the result states that – provided that the Koopman operator satisfies the Assumptions 2.1 and 2.2 below – as both the basis size k as well as the number of measurements m tend to infinity, the matrix K obtained by EDMD converges to the Koopman operator. Since we will utilize this convergence for our results on bilinear reduced order models and optimal control problems, it is summarized below. The detailed proof can be found in [KM17].

Denote by $\mathcal{K}_{k,m}(= K^\top)$ the finite-dimensional approximation of the Koopman operator obtained by EDMD. Here, k is the number of basis functions (i.e. the size of the dictionary) and m the number

of measurements. Before stating the two theorems required for the convergence, we introduce the following two assumptions.

Assumption 2.1. *The basis functions ψ_1, \dots, ψ_k are such that*

$$\mu\{z \in \mathcal{Z} \mid c^\top \psi(z) = 0\} = 0$$

for all $c \in \mathbb{R}^k$, where μ is a given probability distribution according to which the data samples $f(y_1), \dots, f(y_m)$ are drawn and $\mathcal{Z} \subset \mathbb{R}^q$ is the space of all measurements.

This assumption ensures that the measure μ is not supported on a zero level set of a linear combination of the basis functions.

Assumption 2.2. *The following conditions hold:*

1. *The Koopman operator $\mathcal{K}: \mathcal{F} \rightarrow \mathcal{F}$ is bounded.*
2. *The observables ψ_1, \dots, ψ_k defining \mathcal{F}_k (the finite-dimensional representation of \mathcal{F}) are selected from a given orthonormal basis of \mathcal{F} , i.e., $(\psi_i)_{i=1}^\infty$ is an orthonormal basis of \mathcal{F} .*

The convergence of $\mathcal{K}_{k,m}$ to \mathcal{K} is now achieved in two steps. In the first step, convergence of $\mathcal{K}_{k,m}$ to \mathcal{K}_k is shown as the number of samples m tends to infinity. Here, \mathcal{K}_k is the projection of \mathcal{K} onto \mathcal{F}_k . The second step then yields convergence of \mathcal{K}_k towards \mathcal{K} as the basis size k increases.

Theorem 2.3 ([KM17]). *If Assumption 2.1 holds, then we have with probability one for all $\phi \in \mathcal{F}_k$*

$$\lim_{m \rightarrow \infty} \|\mathcal{K}_{k,m}\phi - \mathcal{K}_k\phi\| = 0,$$

where $\|\cdot\|$ is any norm on \mathcal{F}_k . In particular, we obtain

$$\lim_{m \rightarrow \infty} \|\mathcal{K}_{k,m} - \mathcal{K}_k\| = 0,$$

where $\|\cdot\|$ is any operator norm and

$$\lim_{m \rightarrow \infty} \text{dist}(\sigma(\mathcal{K}_{k,m}), \sigma(\mathcal{K}_k)) = 0,$$

where $\sigma(\cdot) \subset \mathbb{C}$ denotes the spectrum of an operator and $\text{dist}(\cdot, \cdot)$ the Hausdorff metric on subsets of \mathbb{C} .

Theorem 2.4 ([KM17]). *Let Assumption 2.2 hold and define the $L_2(\mu)$ projection of a function ϕ onto \mathcal{F}_k by*

$$P_\mu^k \phi = \arg \min_{f \in \mathcal{F}_k} \|f - \phi\|_{L_2(\mu)}.$$

Then the sequence of operators $\mathcal{K}_k P_\mu^k = P_\mu^k \mathcal{K} P_\mu^k$ converges strongly to \mathcal{K} as $k \rightarrow \infty$.

Note that Assumption 2.2 (in particular the boundedness of \mathcal{K}) does not hold for all systems. However, we will assume throughout the remainder of this article that it is satisfied. To summarize, the above theorems yield the following equalities on \mathcal{M} (cf. Figure 1):

$$f \circ \Phi = \mathcal{K} \circ f = B \circ K^\top \circ \Psi \circ f.$$

2.3 Switched system control of PDEs via K-ROMs

The overall goal we pursue is to efficiently solve optimal control problems constrained by PDEs:

$$\begin{aligned}
\min_{u \in \mathcal{U}} J(y, u) &= \min_{u \in \mathcal{U}} \int_{t_0}^{t_e} L(y(\cdot, t)) dt \\
\text{s.t. } \dot{y}(x, t) &= G(y(x, t), u(t)), & (x, t) \in \Omega \times (t_0, t_e], \\
c_1(x, t, u(t)) \frac{\partial y}{\partial n}(x, t) &= c_2(x, t, u(t)) - c_3(x, t, u(t))y(x, t) & (x, t) \in \Gamma \times (t_0, t_e], \\
y(x, t_0) &= y^0(x).
\end{aligned} \tag{1}$$

Here, Ω is the domain of interest, Γ is the boundary, and the functions c_1 , c_2 and c_3 determine the problem specific boundary conditions. The system state is denoted by y , u is the control and $G : \mathbb{R}^d \times \mathbb{R} \rightarrow \mathbb{R}^d$ describes the system dynamics. The time-T map of the system is denoted by:

$$\begin{aligned}
y_{i+1} &= \Phi(y_i, u_i), \\
y_0 &= y^0,
\end{aligned} \tag{2}$$

where we have introduced $y_i = y(x, t_i)$ and $u_i = u(t_i)$ for ease of notation.

For real systems, it is often insufficient to determine a control input a priori. Due to the so-called *plant-model mismatch* – the difference between the dynamics of the real system and the model – the open-loop control input will not be able to control the system as desired or at least be non-optimal. Furthermore, disturbances cannot be taken into account by open-loop control strategies. A remedy to this issue is MPC [GP17], where open-loop problems are solved repeatedly on finite horizons (cf. Figure 2). Using a model of the system dynamics, an open-loop optimal control problem is solved in real-time over a so-called *prediction horizon* of length p . Following [GP17], we consider discrete dynamics. The motivation behind this is that the control is constant over each sample time interval such that it is sufficient to consider the flow map Φ of the continuous dynamics. This results in the following optimal control problem:

$$\begin{aligned}
\min_{u \in \mathbb{R}^p} \sum_{i=s}^{s+p-1} L(y_i) \\
\text{s.t. } y_{i+1} &= \Phi(y_i, u_{i-s+1}) \quad \text{for } i = s, \dots, s+p-1, \\
y_s &= y^s.
\end{aligned} \tag{MPC}$$

The first part of the solution of (MPC) is then applied to the real system while the optimization is repeated with the prediction horizon moving forward by one sample time. (The indexing $i - s + 1$ is required to account for the finite-horizon control and the infinite-horizon state.) For this reason, MPC is also referred to as *moving horizon control* or *receding horizon control*.

According to the approach in [PK17], we now replace the dynamical control system in Problem (MPC) by n_c autonomous systems:

$$\begin{aligned}
y_{i+1} &= \Phi_{u^j}(y_i) \quad \text{for } j = 0, \dots, n_c - 1, \\
y_0 &= y^0,
\end{aligned} \tag{3}$$

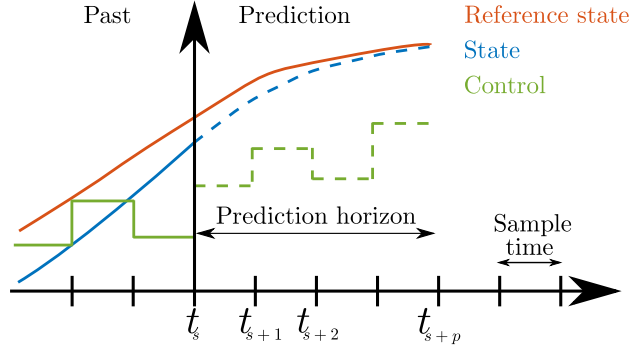


Figure 2: Sketch of the MPC concept for a tracking problem. The step size is $h = t_{s+1} - t_s$.

where the index u^j indicates that the system dynamics Φ_{u^j} correspond to a constant control input u^j . This way Problem (MPC) is transformed into a switched systems problem (cf. [ZA15] for a survey), where the objective is to select the optimal right hand side in each time step:

$$\begin{aligned}
 & \min_{\tau \in \{u^0, \dots, u^{n_c-1}\}^p} \sum_{i=s}^{s+p-1} L(y_i) \\
 \text{s.t. } & y_{i+1} = \Phi_{\tau_{i-s+1}}(y_i) \quad \text{for } i = s, \dots, s+p-1, \\
 & y_s = y^s.
 \end{aligned} \tag{MPCs}$$

In other words, each entry of τ describes which system Φ_{τ_i} to apply in the i^{th} step. Problem (MPCs) is a combinatorial problem that can be solved using dynamic programming [BS15, XA00], for instance.

Solving (MPC) or (MPCs) numerically (e.g. with a finite volume method) can quickly become very expensive such that real-time applicability is not feasible. Furthermore, there are many systems where the dynamics is not explicitly known. In both situations, we can use observations (i.e. data) to approximate the Koopman operator and derive a linear system describing the dynamics of these observations. These could consist of (part of) the system state as well as arbitrary functions of the state such as the lift coefficient of an object within a flow field.

We want to use such a *Koopman operator based reduced order model (K-ROM)* to overcome the issue of large computational cost. To this end, we compute n_c Koopman operators for the n_c different autonomous systems:

$$(\mathcal{K}_{u^j} f)(y) = f(\Phi_{u^j}(y)), \quad j = 0, \dots, n_c - 1.$$

Using EDMD, we can compute an approximation of the individual Koopman operators from observations of the respective systems and thereby derive linear systems for the observations $z = f(y)$:

$$\psi(z_{i+1}) = K_{u^j}^\top \psi(z_i), \quad j = 0, \dots, n_c - 1. \tag{4}$$

These linear dynamics now replace the original differential equation (3) which results in the K-ROM

based formulation of (MPCs):

$$\begin{aligned} & \min_{\hat{\tau} \in \{u^0, \dots, u^{n_c-1}\}^p} \sum_{i=s}^{s+p-1} L_{\mathcal{K}}(\psi(z_i)) \\ \text{s.t. } & \psi(z_{i+1}) = K_{\hat{\tau}_{i-s+1}}^{\top} \psi(z_i) \quad \text{for } i = s, \dots, s+p-1, \\ & z_s = f(y^s). \end{aligned} \tag{K-MPCs}$$

Using the convergence result for the Koopman operator (Theorems 2.3 and 2.4), we can show equality of the optimal solution:

Theorem 2.5 ([PK17]). *Consider Problem (MPCs) and the bilinear approximation (K-MPCs) and let Assumptions 2.1 and 2.2 be satisfied. Furthermore, assume $L(y(t)) = L_{\mathcal{K}}(\psi(z_i))$ for all $t \in [t_0, t_e]$ and the corresponding $i = (t - t_0)/h$. Then (as m and k tend towards infinity, cf. Theorems 2.3 and 2.4) the optimal solutions of (MPCs) and (K-MPCs) are identical, i.e.,*

$$\hat{\tau}^* = \tau^*.$$

Note that the assumption $L(y(t)) = L_{\mathcal{K}}(\psi(z_i))$ is not restrictive in practical settings since we can only consider quantities in the objective function which we can observe. By this approach, we can significantly accelerate the computation which is on the one hand due to the linearity of the model and on the other hand due to the restriction to a small number of observables instead of the full state y . The K-ROM based MPC method is summarized in Algorithm 1.

Algorithm 1 (K-ROM based MPC)

Require: EDMD approximations of n_c Koopman operators; prediction horizon length $p \in \mathbb{N}$.

- 1: **for** $i = 0, 1, 2, \dots$ **do**
 - 2: Obtain measurements of the current system state $z_i = f(y_i)$.
 - 3: Predict the initial condition z_{i+1} for the next MPC optimization problem using the currently active K-ROM using Equation (4).
 - 4: Solve Problem (K-MPCs) with initial condition z_{i+1} on the prediction horizon of length p .
 - 5: At $t = (i + 1)h$, apply the first entry of the solution (i.e. $\hat{\tau}_1^*$) to the system.
 - 6: **end for**
-

3 Continuous control inputs

The switched systems approach presented in Section 2.3 yields speed-ups of several orders of magnitude. However, two drawbacks are that the resulting optimization problem is of combinatorial nature – and is thereby harder to solve – and that the control input is limited to a small number of values. In order to overcome both of these drawbacks, we define the matrices

$$A = K_{u^a}^{\top} \quad \text{and} \quad B = K_{u^b}^{\top} - K_{u^a}^{\top}$$

and introduce the bilinear control system

$$\begin{aligned}\psi(z_{i+1}) &= A\psi(z_i) + B\psi(z_i)\frac{u_i - u^a}{u^b - u^a}, \\ z_0 &= z^0.\end{aligned}\tag{K-ROM}$$

The term bilinear refers to the fact that (K-ROM) contains a term $\psi(z) \cdot u$ but is otherwise linear both in $\psi(z)$ and in u [Eil09]. By choosing $u_i \in [u^a, u^b]$, this system simply interpolates linearly between the two autonomous dynamics corresponding to u^a and u^b . Note that (K-ROM) yields the exact dynamics for $u_i = u^a$ and $u_i = u^b$ due to the convergence result for EDMD. For intermediate values of u , we can exploit the linearity of the Koopman operator.

Theorem 3.1. *Consider a dynamical control system of the form (2) and let \mathcal{K}_{u^a} and \mathcal{K}_{u^b} be the Koopman operators associated with the constant control inputs u^a and u^b .*

Assume that the observation map f is linear and that the system dynamics Φ are linear in u . Then a linear interpolation between the two operators is equal to the Koopman operator for the linear interpolation between the controls u^a and u^b , i.e.

$$\alpha\mathcal{K}_{u^a} + (1 - \alpha)\mathcal{K}_{u^b} = \mathcal{K}_{\alpha u^a + (1 - \alpha)u^b}, \quad \alpha \in [0, 1].$$

Proof. The claim follows directly from the linearity assumptions:

$$\begin{aligned}((\alpha\mathcal{K}_{u^a} + (1 - \alpha)\mathcal{K}_{u^b})f)y &= (\alpha\mathcal{K}_{u^a}f)y + ((1 - \alpha)\mathcal{K}_{u^b}f)y \\ &= \alpha f(\Phi(y, u^a)) + (1 - \alpha)f(\Phi(y, u^b)) \\ &= f(\alpha\Phi(y, u^a) + (1 - \alpha)\Phi(y, u^b)) \\ &= f(\Phi(y, \alpha u^a + (1 - \alpha)u^b)) \\ &= (\mathcal{K}_{\alpha u^a + (1 - \alpha)u^b}f)y.\end{aligned}$$

□

An important consequence of the above theorem is that we can use (K-ROM) to predict the dynamics of the observations z .

Corollary 3.2. *The observations of the state of the dynamical system (2) are equal to the solution of (K-ROM) as m and k tend towards infinity (cf. Theorems 2.3 and 2.4), i.e.*

$$f(\Phi(y_i, u_i)) = P \left(A\psi(f(y_i)) + B\psi(f(y_i))\frac{u_i - u^a}{u^b - u^a} \right).$$

Example 3.3. *Let us consider the following simple example (cf. also [BBPK16]):*

$$\begin{aligned}\dot{y}(t) &= G(y(t), u(t)) = \begin{pmatrix} \mu y_1(t) \\ \lambda(y_2(t) - (y_1(t))^2) + u^x(t) \end{pmatrix}, \\ y(0) &= y^0.\end{aligned}\tag{5}$$

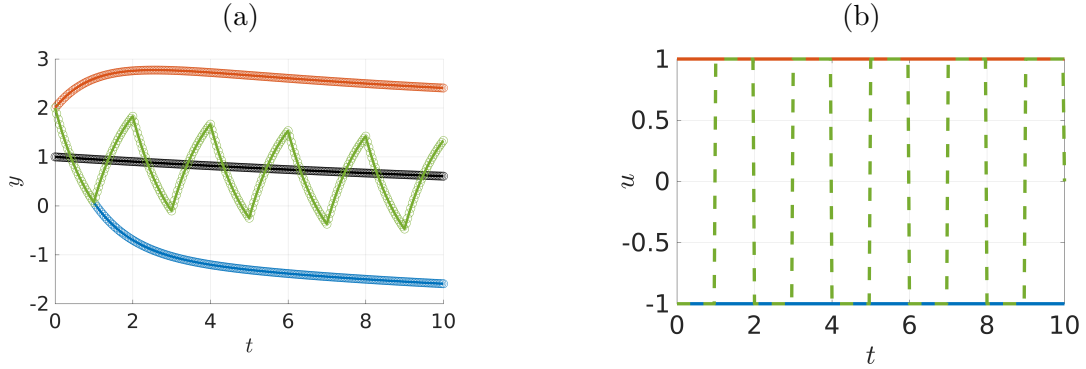


Figure 3: (a) Trajectories of y_2 of two different autonomous systems ($u^a = -1$ (blue) and $u^b = 1$ (orange)) with starting point $y^0 = (1, 2)^\top$ and linear control input ($\chi = 1$) according to (b). The y_2 trajectory of the switched system is shown in green. The lines are the solution of Equation (6) and the circles the solution of the corresponding K-ROM. The first component y_1 is identical in all cases and is shown in black.

Here we have additionally introduced a factor χ in order to study the relevance of the linearity assumption for the control input. By restricting ourselves to n_c constant controls, we can transform the system into n_c autonomous systems:

$$\begin{aligned} \dot{y}(t) &= G_{w^j}(y(t)) = \begin{pmatrix} \mu y_1(t) \\ \lambda(y_2(t) - (y_1(t))^2) \end{pmatrix} + \begin{pmatrix} 0 \\ (u^j)^\chi \end{pmatrix}, \quad j = 0, \dots, n_c - 1, \\ y(0) &= y^0. \end{aligned} \quad (6)$$

Since this is a finite-dimensional system, we set $f(y) = y$ and observe the full state such that (K-ROM) is a reduced model for y . In a first step, we reproduce the dynamics of the two systems with $u^a = -1$ and $u^b = 1$ and a switched system with constant switching times (cf. Figure 3 and also [PK17]). For the system (6), we can use EDMD to exactly compute the Koopman operator [BBPK16]. Consequently, we observe almost perfect agreement between the ODE solution and the K-ROM approximation. For details on the numerical approximation of \mathcal{K}_{-1} and \mathcal{K}_1 , see Table 1 on p. 14.

In the next step, we compare the solutions of the ODE (5) and the K-ROM approximation for intermediate values of u , cf. Figure 4. We see that in accordance with Theorem 3.1, we again observe a very high accuracy.

Finally, we study solutions with $\chi > 1$, i.e. nonlinear control inputs. We here construct (K-ROM) from the operators \mathcal{K}_0 and \mathcal{K}_1 . Due to the choice $u^a = 0$ and $u^b = 1$, the exponent χ does not influence these two solutions and hence, all K-ROM solutions are identical. We observe that the very good agreement from the linear case $\chi = 1$ can not be preserved, cf. Figure 5, where the y_2 trajectories are shown in (a) and the relative error

$$\epsilon_{rel}(t) = \frac{|y_2^{K-ROM}(t) - y_2^{ODE}(t)|}{|y_2^{ODE}(t)|}$$

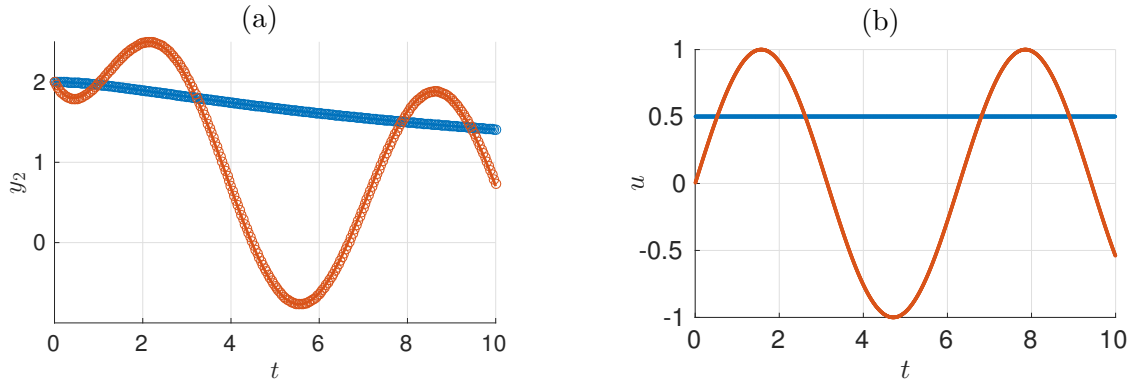


Figure 4: Similar to Figure 3 but with continuous control inputs, i.e. comparison between (5) and the K-ROM approximation.

is shown in (b). However – depending on how well the control dependency can be linearized – we still have acceptable accuracy and a qualitative prediction is possible. Consequently, the K-ROM can be interpreted as being an implicit local linearization.

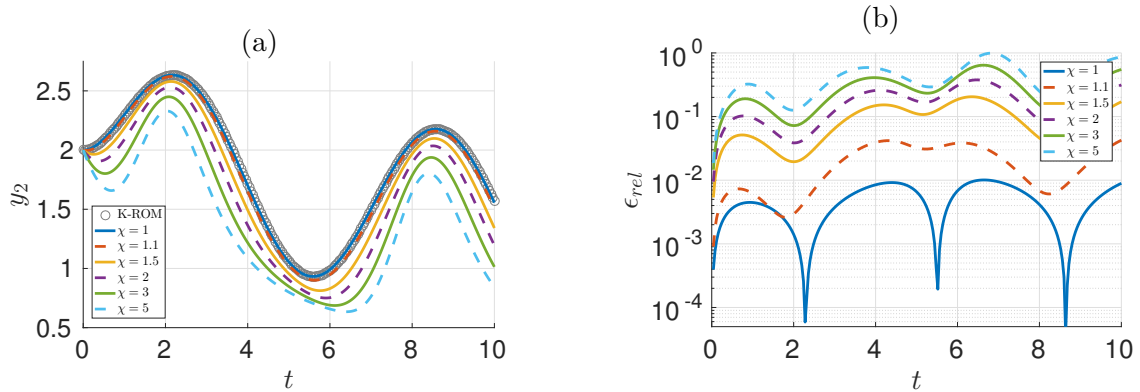


Figure 5: (a) Comparison between the solutions of the ODE system (5) and (K-ROM) for $u(t) = 0.5 + 0.5 \sin(t)$ and varying values of χ . (b) Relative error between the respective solutions.

4 PDE constraints

The reduced order model (K-ROM) enables us to approximate a nonlinear, infinite-dimensional control system by a finite-dimensional bilinear system in a very efficient manner. Due to the increased step size of the K-ROM and the linearity, we already observe a significant speed-up. Furthermore, such a bilinear model allows us to use solution methods from bilinear control theory (see [PY08, Ell09] for an introduction), which additionally accelerates the computations. The approach shows its full potential when considering PDEs (cf. Table 1 for a summary), which we will show in the following using two examples.

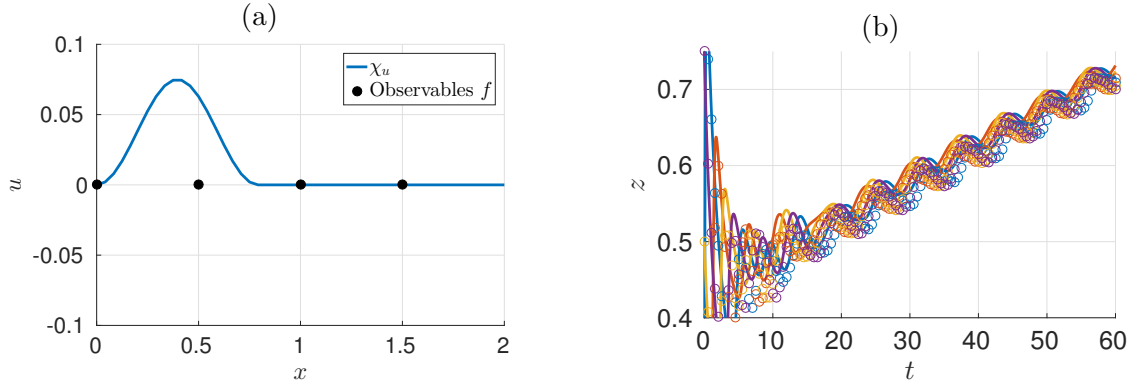


Figure 6: (a) Shape function χ_u and observables f . (b) Comparison between the solutions of the 1D Burgers PDE and the K-ROM approximation for $u(t) = -0.025 + 0.05 \sin(t)$.

1D Burgers equation. As our first example we consider the 1D Burgers equation with periodic boundary conditions and $\nu = 0.01$, and we consider a distributed control using the shape function χ_u (see Figure 6 (a)):

$$\begin{aligned} \dot{y}(x, t) - \nu \Delta y(x, t) + y(x, t) \nabla y(x, t) &= u(t) \chi_u(x), \\ y(x, 0) &= y^0(x). \end{aligned}$$

In contrast to the ODE case, we do not observe the full state but only certain points in space (the black dots in Figure 6 (a)), i.e.,

$$z_i = f(y(\cdot, t_i)) = (y(0, t_i), y(0.5, t_i), y(1, t_i), y(1.5, t_i))^\top,$$

and we construct the K-ROM for these observations from data collected at $u^a = -0.025$ and $u^b = 0.075$ and two different initial conditions, respectively. In Figure 6 (b) the comparison between the observation of the PDE solution and the K-ROM approximation is shown for a sinusoidal control. We see that the error is larger than in the ODE example 3.3 but that the qualitative agreement is still very good. Due to the linearity and the lower dimension of the K-ROM (35), we achieve a speed-up of approximately 100 (cf. Table 1).

2D Navier–Stokes equations. As a second example, we consider the flow of a fluid around a cylinder described by the 2D incompressible Navier–Stokes equations at a Reynolds number of $Re = 100$ (see Figure 7 (a) for the problem setup):

$$\begin{aligned} \dot{y}(x, t) + y(x, t) \cdot \nabla y(x, t) &= \nabla p(x, t) + \frac{1}{Re} \Delta y(x, t), \\ \nabla \cdot y(x, t) &= 0, \\ y(x, 0) &= y^0(x), \end{aligned}$$

where y is the flow velocity and p is the pressure. The system is controlled via rotation of the cylinder, i.e., $u(t)$ is the angular velocity. The uncontrolled system possesses a periodic solution, the well-known *von Kármán vortex street*.

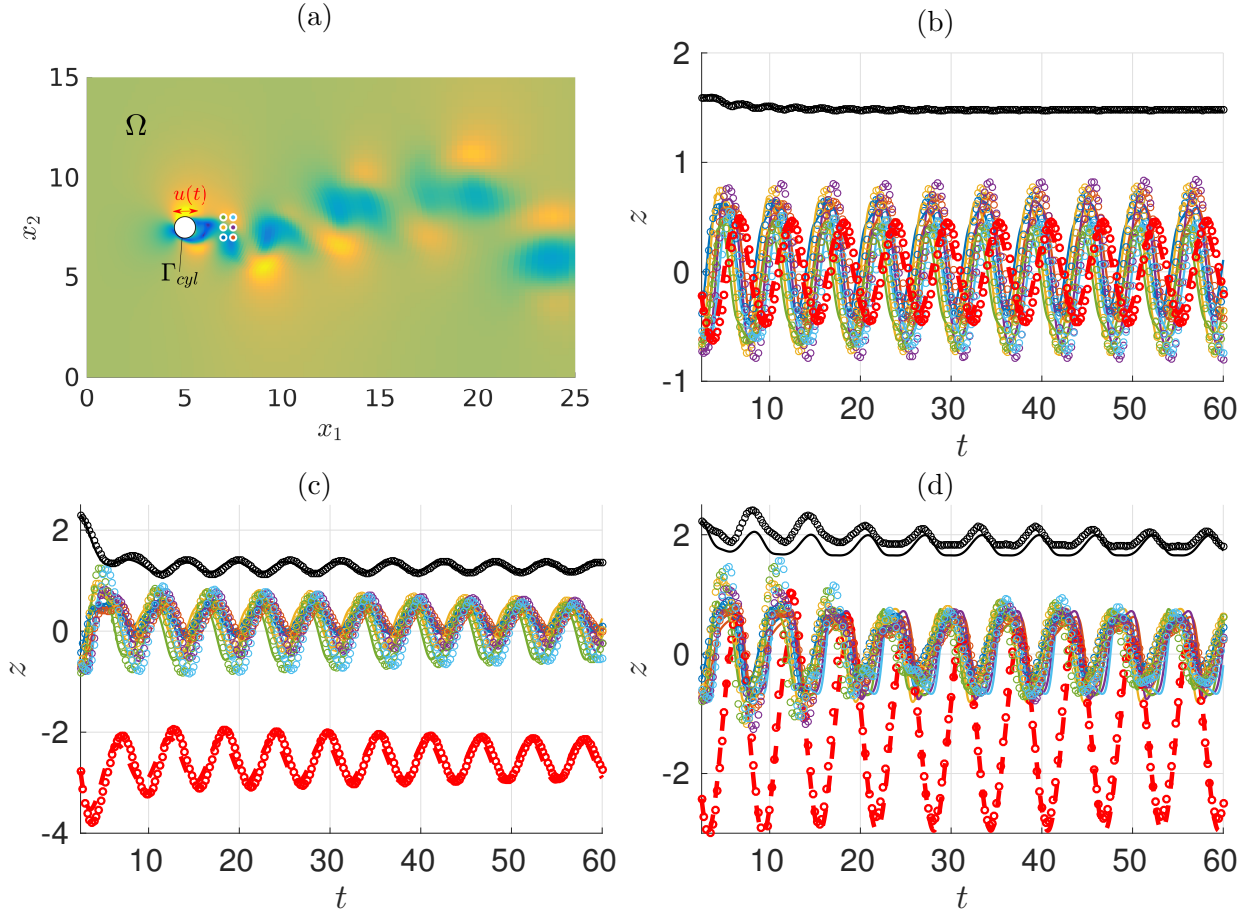


Figure 7: (a) Sketch of the problem setting. The domain is denoted by Ω and the boundary of the cylinder by Γ_{cyl} . (b) and (c) Observation of the PDE solution and K-ROM approximation for $u^a = 0$ and $u^b = 2$, respectively. The lift is shown by the dashed red line, the drag is shown in black and the remaining lines are the vertical velocities at the six positions shown in (a). (d) Observation of the PDE solution and K-ROM approximation for $u(t) = 1 + \sin(t)$.

We now follow the same procedure as in the previous example. Instead of observing the full state, we observe the lift C_l and the drag C_d of the cylinder:

$$C_l(t) = \int_{\Gamma_{cyl}} p_2(x, t) dx, \quad C_d(t) = \int_{\Gamma_{cyl}} p_1(x, t) dx,$$

where p_i is the projection of the pressure onto the i^{th} spatial direction. Additionally, we observe the vertical velocity at six different positions (x_1, \dots, x_6) in the cylinder wake (see Figure 7 (a)):

$$z_i = f((y(\cdot, t_i), p(\cdot, t_i))) = (C_l(t_i), C_d(t_i), y_2(x_1, t_i), \dots, y_2(x_6, t_i))^{\top}.$$

Figures 7 (b) and 7 (c) show a comparison between the PDE and the K-ROM solution for constant control inputs $u^a = 0$ and $u^b = 2$. We see that in both cases, the solutions agree remarkably well,

Table 1: Numerical setup and efficiency analysis for different dynamical systems.

Problem	ODE (5)	1D Burgers	2D NSE
Time step h	0.04	0.5	0.25
Sampling of the data	Separate trajectories for the individual \mathcal{K}_{u^j} (cf. Figure 3 (a))	Two simulations (60s) with different initial conditions y^0 , fixed switching sequence	One simulation (1500s) with random switching (concerning both switching time and order)
Dictionary ψ : Monomials of order	2	3	2
Dimension of z	2	4	8
Dimension of K	6	35	45
K-ROM speed-up	≈ 17	≈ 100	$\approx 7.5 \cdot 10^4$

considering that the NSE solver uses a finite volume discretization with 22.000 cells and the K-ROM is a 45-dimensional linear model. This results in a speed-up of approximately 75,000 (OpenFOAM [JJT07] vs. MATLAB). Figure 7 (d) shows a comparison of the solutions for a sinusoidal control and we see that the agreement is still satisfactory although the system does not depend linearly on the control such that the assumptions of Theorem 3.1 are violated.

5 Model predictive control

We have seen in the previous section that we can use (K-ROM) to approximate a nonlinear, infinite-dimensional control system by a finite-dimensional bilinear system in a very efficient manner. However, since the accuracy can very likely not always be expected to be this good for finite amounts of data and finite-dimensional dictionaries ψ , we now embed the above approach in an MPC framework such that we only require high accuracy on short time intervals. To this end, we formulate the K-ROM approximation of the original closed-loop problem (MPC):

$$\min_{u \in \mathcal{U}} \sum_{i=s}^{s+p-1} L_{\mathcal{K}}(\psi(z_i)) \tag{K-MPC}$$

$$\psi(z_{i+1}) = A\psi(z_i) + B\psi(z_i) \frac{u_{i-s+1} - u^a}{u^b - u^a} \quad \text{for } i = s, \dots, s+p-1,$$

$$z_s = f(y^s).$$

The resulting MPC algorithm is very similar to Algorithm 1, but now we have to solve Problem (K-MPC) instead of (K-MPCs) in step 4. Equality of the solutions follows from Theorem 3.1 and Corollary 3.2.

Theorem 5.1. *Consider Problem (MPC) and the approximation (K-MPC) and let Assumptions 2.1 and 2.2 be satisfied. Furthermore, assume $L(y(t)) = L_{\mathcal{K}}(\psi(z_i))$ for all $t \in [t_0, t_e]$ and the*

corresponding $i = (t - t_0)/h$. Then (as m and k tend towards infinity, cf. Theorems 2.3 and 2.4), Problems (K-MPC) and (MPC) possess the same solution.

Problem (K-MPC) can now be solved very efficiently using methods known from bilinear systems theory [PY08]. Since the focus of this article is on the development of the K-ROM, we here simply solve the problem using MATLAB's internal SQP solver.

To demonstrate the effectiveness of the K-ROM MPC approach, we again consider the example of the 2D Navier–Stokes equations. The goal is to control the lift by rotating the cylinder. Since the lift coefficient is one of the observables, we simply have to track the corresponding entry of z in the MPC problem:

$$\min_{u \in [-2, 2]^p} \sum_{i=s}^{s+p-1} (z_{i,1} - z_i^{\text{opt}})^2$$

$$\psi(z_{i+1}) = A\psi(z_i) + B\psi(z_i) \frac{u_{i-s+1} - u^a}{u^b - u^a} \quad \text{for } i = s, \dots, s+p-1,$$

$$z_s = f(y(\cdot, t_s), p(\cdot, t_i)).$$

We want to allow control inputs between -2 and 2 and since the control does not enter linearly into the system, we create two K-ROMs which are *localized* in the control domain. This means that we approximate the Koopman operators \mathcal{K}_{-2} , \mathcal{K}_0 and \mathcal{K}_2 and construct two reduced models of the form (K-ROM), one of which is valid on the interval $[-2, 0)$ and the other one on the interval $[0, 2]$. Similar ideas of localized reduced order models are often used in the *reduced basis* community (cf. e.g. [AHKO12, BDPV17]).

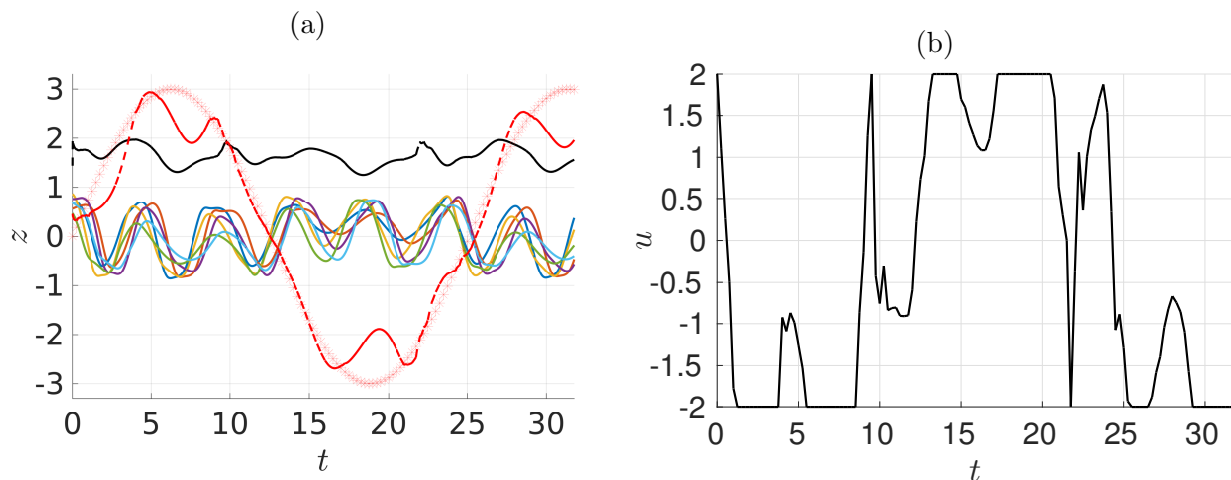


Figure 8: (a) Trajectory of the observable z corresponding to the control shown in (b), the reference trajectory z^{opt} is shown by the red stars. (b) The control computed by the K-ROM MPC framework.

Figure 8 shows the MPC solution for a sinusoidal reference trajectory of the lift. We see in

Figure 8 (a) that this curve can be tracked very well except in situations where the control bounds are active which is the case when the lift is either very large or very low (cf. Figure 8 (b)).

6 Conclusion

We have presented a new approach for Koopman operator based reduced order models which can be used for real-time control of nonlinear PDEs. Two Koopman operators are approximated via EDMD at different constant control inputs. Intermediate control values can be approximated by linearly interpolating between these two operators which yields a bilinear control system. If the original system depends linearly on the control input, one can prove that this approach results in the true optimum of the optimal control problem. However, as examples show, the approach leads to very good results even in situations where this assumption does not hold. In this case, the control approach can be interpreted as an implicit local linearization.

Due to the larger step sizes and the linearity of the K-ROM, the reduced model can be solved significantly faster, in the case of the 2D Navier–Stokes equations by a factor of approximately 75,000. An additional benefit is that since the model is bilinear, we can use efficient solution methods for the reduced control problem.

One further direction of research is to develop stronger statements about the error for the K-ROM approach, e.g. concerning the basis size or the required data. To this end, it might also be interesting to study the influence of the assumptions on the dynamical system in order to obtain convergence EDMD towards the Koopman operator. From a control theoretic perspective, it would be very interesting to investigate whether the notion of controllability can be carried over to nonlinear systems. Moreover, feedback controllers for bilinear systems could help to further improve the efficiency over MPC. In terms of numerical efficiency, automated methods for choosing appropriate basis functions for the system dynamics (e.g., via dictionary learning [LDBK17]) could help to further improve the range of applicability. When applied flow control problems, higher Reynolds numbers will certainly introduce additional challenges for the K-ROM approach.

References

- [AHKO12] F. Albrecht, B. Haasdonk, S. Kaulmann, and M. Ohlberger. The localized reduced basis multiscale method. In *Proceedings of ALGORITHMY 2012*, pages 393–403, 2012.
- [AM17] H. Arbabi and I. Mezić. Ergodic theory, dynamic mode decomposition and computation of spectral properties of the Koopman operator. *arXiv:1611.06664v6*, 2017.
- [BBPK16] S. L. Brunton, B. W. Brunton, J. L. Proctor, and J. N. Kutz. Koopman invariant subspaces and finite linear representations of nonlinear dynamical systems for control. *PLoS ONE*, 11(2):1–19, 2016.
- [BC08] M. Bergmann and L. Cordier. Optimal control of the cylinder wake in the laminar regime by trust-region methods and POD reduced-order models. *Journal of Computational Physics*, 227(16):7813–7840, 2008.
- [BDK74] C. Bruni, G. DiPillo, and G. Koch. Bilinear Systems: An Appealing Class of Nearly Linear Systems in Theory and Applications. *IEEE Transactions on Automatic Control*, 19(4):334–348, 1974.

- [BDPV17] D. Beermann, M. Dellnitz, S. Peitz, and S. Volkwein. Set-Oriented Multiobjective Optimal Control of PDEs using Proper Orthogonal Decomposition. *Submitted*, 2017.
- [BGW15] P. Benner, S. Gugercin, and K. Willcox. A Survey of Projection-Based Model Reduction Methods for Parametric Dynamical Systems. *SIAM Review*, 57(4):483–531, 2015.
- [BMM12] M. Budišić, R. Mohr, and I. Mezić. Applied Koopmanism. *Chaos*, 22, 2012.
- [BN15] S. L. Brunton and B. R. Noack. Closed-Loop Turbulence Control: Progress and Challenges. *Applied Mechanics Reviews*, 67(5):1–48, 2015.
- [BS15] R. E. Bellmann and E. D. Stuart. *Applied dynamic programming*. Princeton University Press, 2015.
- [DBN17] T. Duriez, S. L. Brunton, and B. R. Noack. *Machine Learning Control Taming Nonlinear Dynamics and Turbulence*. Springer, 2017.
- [Ell09] D. L. Elliott. *Bilinear Control Systems - Matrices in Action*. Springer Science + Business Media, 2009.
- [Fah00] M. Fahl. *Trust-region Methods for Flow Control based on Reduced Order Modelling*. Phd thesis, University of Trier, 2000.
- [GP17] L. Grüne and J. Pannek. *Nonlinear Model Predictive Control*. Springer International Publishing, 2 edition, 2017.
- [HV05] M. Hinze and S. Volkwein. Proper Orthogonal Decomposition Surrogate Models for Nonlinear Dynamical Systems: Error Estimates and Suboptimal Control. In P. Benner, D. C. Sorensen, and V. Mehrmann, editors, *Reduction of Large-Scale Systems*, volume 45, pages 261–306. Springer Berlin Heidelberg, 2005.
- [JJT07] H. Jasak, A. Jemcov, and Z. Tukovic. OpenFOAM : A C++ Library for Complex Physics Simulations. *International Workshop on Coupled Methods in Numerical Dynamics*, pages 1–20, 2007.
- [KGPS16] S. Klus, P. Gelß, S. Peitz, and C. Schütte. Tensor-based dynamic mode decomposition. *arXiv:1606.06625*, 2016.
- [KKB17] E. Kaiser, J. N. Kutz, and S. L. Brunton. Data-driven discovery of Koopman eigenfunctions for control. *arXiv:1707.0114*, 2017.
- [KKS16] S. Klus, P. Koltai, and C. Schütte. On the numerical approximation of the Perron-Frobenius and Koopman operator. *Journal of Computational Dynamics*, 3(1):51–79, 2016.
- [KM16] M. Korda and I. Mezić. Linear predictors for nonlinear dynamical systems: Koopman operator meets model predictive control. *arXiv:1611.03537*, 2016.
- [KM17] M. Korda and I. Mezić. On Convergence of Extended Dynamic Mode Decomposition to the Koopman Operator. *arXiv:1703.04680*, 2017.
- [KNK⁺17] S. Klus, F. Nüske, P. Koltai, H. Wu, I. Kevrekidis, C. Schütte, and F. Noé. Data-driven model reduction and transfer operator approximation. *ArXiv e-prints*, 2017.
- [Koo31] B. O. Koopman. Hamiltonian Systems and Transformations in Hilbert Space. *Proceedings of the National Academy of Sciences*, 17(5):315–318, 1931.
- [Kut17] J. N. Kutz. Deep learning in fluid dynamics. *Journal of Fluid Mechanics*, 814:1–4, 2017.

- [KV99] K. Kunisch and S. Volkwein. Control of the Burgers Equation by a Reduced-Order Approach Using Proper Orthogonal Decomposition. *Journal of Optimization Theory and Applications*, 102(2):345–371, 1999.
- [LDBK17] Q. Li, F. Dietrich, E. M. Bollt, and I. G. Kevrekidis. Extended dynamic mode decomposition with dictionary learning: a data-driven adaptive spectral decomposition of the Koopman operator. *arXiv:1707.00225v1*, 2017.
- [LM94] A. Lasota and M. C. Mackey. *Chaos, fractals, and noise: Stochastic aspects of dynamics*, volume 97 of *Applied Mathematical Sciences*. Springer, 2nd edition, 1994.
- [LMQR14] T. Lassila, A. Manzoni, A. Quarteroni, and G. Rozza. Model order reduction in fluid dynamics : challenges and perspectives. In A. Quarteroni and G. Rozza, editors, *Reduced Order Methods for Modeling and Computational Reduction*, pages 235–273. Springer, Cham, 2014.
- [MB04] I. Mezić and A. Banaszuk. Comparison of systems with complex behavior. *Physica D: Nonlinear Phenomena*, 197:101–133, 2004.
- [Mez05] I. Mezić. Spectral Properties of Dynamical Systems, Model Reduction and Decompositions. *Nonlinear Dynamics*, 41:309–325, 2005.
- [Mez13] I. Mezić. Analysis of Fluid Flows via Spectral Properties of the Koopman Operator. *Annual Review of Fluid Mechanics*, 45:357–378, 2013.
- [PBK15] J. L. Proctor, S. L. Brunton, and J. N. Kutz. Dynamic mode decomposition with control. *SIAM Journal on Applied Dynamical Systems*, 15(1):142–161, 2015.
- [PBK16] J. L. Proctor, S. L. Brunton, and J. N. Kutz. Generalizing Koopman Theory to allow for inputs and control. *arXiv:1602.07647v1*, 2016.
- [Pei17] S. Peitz. *Exploiting Structure in Multiobjective Optimization and Optimal Control*. PhD thesis, Paderborn University, 2017.
- [PK17] S. Peitz and S. Klus. Koopman operator-based model reduction for switched-system control of PDEs. *arXiv:1710:06759*, 2017.
- [PY08] P. M. Pardalos and V. Yatsenko. *Optimization and Control of Bilinear Systems*. Springer, 2008.
- [QGVW16] E. Qian, M. Grepl, K. Veroy, and K. Willcox. A Certified Trust Region Reduced Basis Approach to PDE-Constrained Optimization. *ACDL Technical Report TR16-3*, 2016.
- [RMB⁺09] C. W. Rowley, I. Mezić, S. Bagheri, P. Schlatter, and D. S. Henningson. Spectral analysis of nonlinear flows. *Journal of Fluid Mechanics*, 641:115–127, 2009.
- [Row05] C. W. Rowley. Model Reduction for Fluids, Using Balanced Proper Orthogonal Decomposition. *International Journal of Bifurcation and Chaos*, 15(3):997–1013, 2005.
- [RTV17] S. Rogg, S. Trenz, and S. Volkwein. Trust-Region POD using A-Posteriori Error Estimation for Semilinear Parabolic Optimal Control Problems. <http://kops.uni-konstanz.de/handle/123456789/38240>, 2017.
- [Sch10] P. J. Schmid. Dynamic mode decomposition of numerical and experimental data. *Journal of Fluid Mechanics*, 656:5–28, 2010.
- [Sir87] L. Sirovich. Turbulence and the dynamics of coherent structures part I: coherent structures. *Quarterly of Applied Mathematics*, XLV(3):561–571, 1987.

- [SOBG16] B. Stellato, S. Ober-Blöbaum, and P. J. Goulart. Optimal Control of Switching Times in Switched Linear Systems. In *IEEE 55th Conference on Decision and Control*, pages 7228–7233, 2016.
- [TBD⁺17] K. Taira, S. L. Brunton, S. T. M. Dawson, C. W. Rowley, T. Colonius, B. J. McKeon, O. T. Schmidt, S. Gordeyev, V. Theofilis, and L. S. Ukeiley. Modal Analysis of Fluid Flows: An Overview. *AIAA Journal*, 55(12):4013–4041, 2017.
- [TRL⁺14] J. H. Tu, C. W. Rowley, D. M. Luchtenburg, S. L. Brunton, and J. N. Kutz. On Dynamic Mode Decomposition: Theory and Applications. *Journal of Computational Dynamics*, 1(2):391–421, 2014.
- [TV09] F. Tröltzsch and S. Volkwein. POD a-posteriori error estimates for linear-quadratic optimal control problems. *Computational Optimization and Applications*, 44(1):83–115, 2009.
- [WKR15] M. O. Williams, I. G. Kevrekidis, and C. W. Rowley. A data-driven approximation of the Koopman operator: Extending dynamic mode decomposition. *Journal of Nonlinear Science*, 25(6):1307–1346, 2015.
- [XA00] X. Xu and P. Antsaklis. A dynamic programming approach for optimal control of switched systems. In *Proceedings of the 39th IEEE Conference on Decision and Control*, pages 1822–1827, 2000.
- [ZA15] F. Zhu and P. J. Antsaklis. Optimal control of hybrid switched systems: A brief survey. *Discrete Event Dynamic Systems*, 25(3):345–364, 2015.